Research in Astronomy and Astrophysics, 24:125016 (8pp), 2024 December https://doi.org/10.1088/1674-4527/ad94ce

Constrain the Jerk Parameters with DESI 2024 Data

Jia-Wei Wu[1] and Kun-Yuan Hong[2]
[1] School of Physics and Astronomy, Sun Yat-sen University, Zhuhai 519082, China; wujw68@mail2.sysu.edu.cn
[2] Department of Physics and Astronomy, University College London, Gower Street, London, WC1E 6BT, UK; kunyuan.hong.21@ucl.ac.uk
Received 2024 September 14; revised 2024 November 12; accepted 2024 November 18; published 2024 December 9

Abstract

The deceleration coefficient q and the jerk coefficient j obtained by the Taylor expansion of the scale factor $a(t)$ play an important role in the study of cosmology. The current value of these coefficients for a cosmological model reflects the transition time between the phases dominated by dark energy and matter and can be used to determine if and how much the universe is decelerating. Thus, these coefficient values offer a way of constraining a particular cosmology model. Research based on this scenario was completed by Orlando Luongo and Marco Muccino. However, some approaches in this method should be tested prudently because some conditions such as $\frac{dd_L}{dz} > 0$ and $\frac{dH}{dz} > 0$ may not be guaranteed. In this study, we used the MAPAge model to reconstruct the jerk parameters (q_0 and j_0) with DESI 2024 data. Using the MAPAge model ensures particular physical circumstances are satisfied in the approach of determining the jerk parameters. Compared to the previous method, which used the Taylor expansion series q_0, j_0, and s_0 as model-independent parameters, we obtained more physical and slightly different results for the jerk parameters. Our results suggest that the DESI 2024 BAO data set favours different jerk parameters compared to the jerk parameters in the standard ΛCDM model.

Key words: (cosmology:) dark energy – (cosmology:) large-scale structure of universe – (cosmology:) cosmological parameters

1. Introduction

A cosmological model with a space curvature of zero, cold dark matter (CDM), and dark energy that does not evolve with time is called the standard cosmological model or ΛCDM model. ΛCDM model has been a great success in the past decades (Baumann 2009; Eisenstein & Hu 1998), but problems including the Hubble tension and the σ_8 tension remain unsolved under the theory of ΛCDM model (Perivolaropoulos & Skara 2022; Riess et al. 2022; Hu & Wang 2023). Therefore, a number of alternative schemes were proposed to solve these problems (Bamba et al. 2012; Perivolaropoulos & Skara 2022; Di Valentino et al. 2021). Recently, with the release of DESI 2024 high-precision data, a series of model-checking studies have been conducted to verify different cosmological models (Adame et al. 2024; Calderon et al. 2024; Carloni et al. 2024; Colgáin et al. 2024; Marina et al. 2024; Yang et al. 2024). One of the methods to verify the feasibility of each model is through the deceleration and the jerk hierarchical terms in the Taylor expansion of the scale factor $a(t)$ (Visser 2004; Luongo & Muccino 2024). However, some approaches in this method should be tested prudently because some conditions such as $\frac{dd_L}{dz} > 0$ and $\frac{dH}{dz} > 0$ may not be guaranteed (Huang 2020). In this paper, we used an alternative model to verify this fitting and ensure that certain physical conditions are fulfilled.

To access the fitting result of the deceleration coefficient q_0 and the jerk coefficient j_0 (the subscript 0 indicates it is the current values), we consider using the "More Accurate Parameterization based on cosmic Age (MAPAge)" model (Huang et al. 2021b) for the fitting. Specifically, in the MAPAge model, a new degree of freedom η_2 is included to improve the fitting accuracy of the "Parameterization based on cosmic Age (PAge)" model suggested by Huang (2020) to approximate a broad class of beyond ΛCDM models, with a typical accuracy $\sim$1% in angular diameter distances at redshift $z \lesssim 10$. The study shows that as long as the model's parameters are limited, a series of cosmological conditions can be guaranteed. These will be exhibited in detail later in our article.

In this research, we processed the r_d parameter as a constant spanning within the range [144, 152] Mpc to ensure both the Planck satellite and DESI-BAO expectations fall within, with a fixed step, $\delta r_d = 2$ Mpc, to make an effective comparison with the early research done by Orlando Luongo and Marco Muccino. (Luongo & Muccino 2024; Brieden et al. 2023). The Monte Carlo Markov chain (MCMC) analyses were used to obtain the parameters in the MAPAge model to fit the optimal values of q_0 and j_0. Incorporating three combinations of data catalogs: the first BAO with observational Hubble data, the second BAO with type Ia supernovae, and the last includes all three data sets. For comparison, similar analyses are done

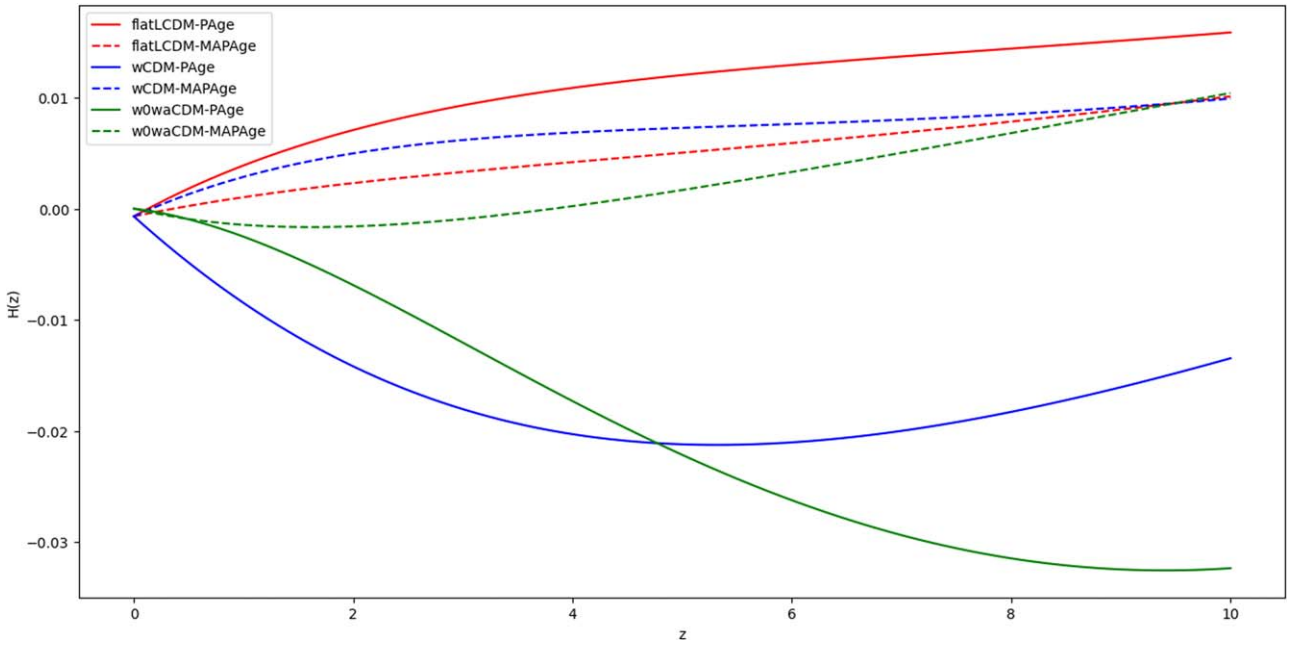

Figure 1. PAge approximation and MAPAge approximation: relative errors of Hubble parameter. Model parameters are given in Table 1.

Table 1
Fitting Parameters and Maximum Relative Error of MAPAge and PAge Models Corresponding to Some Models

Model	Model Params.	PAge Params.	MAPAge Params.	$\max\left\lvert\frac{\Delta H}{H}\right\rvert_{\rm PAge}$	$\max\left\lvert\frac{\Delta H}{H}\right\rvert_{\rm MAPAge}$
ΛCDM	$\Omega_m = 0.3$	$p_{\rm age} = 0.973$, $\eta = 0.439$	$p_{\rm age} = 0.970$, $\eta = 0.393$, $\eta_2 = 0.0510$	9.37×10^{-3}	5.79×10^{-3}
wCDM	$\Omega_m = 0.3$, $\omega = -1.2$	$p_{\rm age} = 0.987$, $\eta = 0.518$	$p_{\rm age} = 0.998$, $\eta = 0.708$, $\eta_2 = -0.211$	1.73×10^{-2}	5.91×10^{-3}
CPL	$\Omega_m = 0.3$, $\omega_0 = -1$, $\omega_a = 0.3$	$p_{\rm age} = 0.957$, $\eta = 0.362$	$p_{\rm age} = 0.956$, $\eta = 0.347$, $\eta_2 = 0.0168$	1.98×10^{-2}	5.83×10^{-3}

Note. PAge and MAPAge models are both approximations under low redshift, so the redshift range of the Hubble parameter studied in this table is in $z < 10$.

with the Chevallier–Polarski–Linder (CPL) model. The code we used can be found in Huang et al. (2024)

We rebuilt the deceleration parameter and the jerk parameter with the MAPAge model in the MCMC analyses, the result obtained is similar to the method which uses Taylor expansion of $a(t)$ Luongo & Muccino (2024). However, a slight difference appears which will be discussed. We also conclude that dynamical dark energy better adapts to this catalog of BAO as previous studies have shown (Adame et al. 2024). Our results regard the concordance model with severe disfavor both on the deceleration parameter and the jerk parameter.

The remainder of this paper is organized as follows: In Section 2, we described the MAPAge model and the parameters that need to be constrained. In Section 3, we report our data set and its corresponding processing details. In Section 4, the results are illustrated and the physical consequences of the analyses are discussed. Also, comparisons between different models are made. Finally, the conclusions are highlighted in Section 5.

2. Model

In the PAge model (Huang 2020), two conditions were assumed: (i) the universe is dominated by matter at high redshift $z \gg 1$, and (ii) the product of the cosmological time t and the Hubble expansion rate H can be approximated as a quadratic function of t. These assumptions lead to the parameterization of the Universe expansion rate H as:

$$\frac{H}{H_0} = 1 + \frac{2}{3}\left(1 - \eta\frac{H_0 t}{p_{\rm age}}\right)\left(\frac{1}{H_0 t} - \frac{1}{p_{\rm age}}\right), \tag{1}$$

where $p_{\rm age} = H_0 t_0$ is the product of the Hubble constant H_0 and the current age of the universe t_0 and the phenomenological parameter η can be regarded as a quadratic fitting parameter. If the value of η is required to be less than 1, the physical conditions $\frac{dd_L}{dz} > 0$ and $\frac{dH}{dz} > 0$ can be guaranteed. It has been shown that the fitting errors of the distance moduli are typically 1% at $z \lesssim 10$ (Luo et al. 2020; Huang et al. 2021a) and such

Table 2
The Cosmological Coefficients Inferred from the Theoretical Cosmological Sets for Each Model (Luongo & Muccino 2024; Aghanim et al. 2020; Adame et al. 2024)

Model	Ω_m	w (w_0)	w_a	Bounds	q_0	j_0
ΛCDM	0.310 ± 0.007	-1	⋯	Planck	-0.535 ± 0.011	1
	0.307 ± 0.005	-1	⋯	DESI	-0.540 ± 0.008	1
wCDM	0.310 ± 0.007	-0.960 ± 0.080	⋯	Planck	-0.494 ± 0.093	0.881 ± 0.230
	0.317 ± 0.007	-0.967 ± 0.024	⋯	DESI	-0.491 ± 0.034	0.902 ± 0.070
CPL	0.310 ± 0.007	-0.957 ± 0.080	$-0.290^{+0.320}_{-0.260}$	Planck	-0.490 ± 0.093	$0.572^{+0.563}_{-0.501}$
	0.316 ± 0.007	-0.727 ± 0.067	$-1.050^{+0.310}_{-0.270}$	DESI	-0.246 ± 0.076	$-0.688^{+0.428}_{-0.387}$

Note. Different observation items often assume that a certain model is correct and then measure the relevant physical quantities to study the self-consistency of various models. The results show that these observations maintained the self-consistency of the appropriate models. Here, the measured values from Planck and DESI are given to make a comparison with the following values of our works.

Table 3
The DESI-BAO samples with Tracers, Effective Redshifts $z_{\rm eff}$, and Ratios d_M/r_d, d_H/r_d, and d_V/r_d (Adame et al. 2024)

Tracer	$z_{\rm eff}$	d_M/r_d	d_H/r_d	d_V/r_d or r
BGS	0.30	⋯	⋯	7.93 ± 0.15
LRG	0.51	13.62 ± 0.25	20.98 ± 0.61	-0.445
LRG	0.71	16.85 ± 0.32	20.08 ± 0.60	-0.420
LRG+ELG	0.93	21.71 ± 0.28	17.88 ± 0.35	-0.389
ELG	1.32	27.79 ± 0.69	13.82 ± 0.42	-0.444
QSO	1.49	⋯	⋯	26.07 ± 0.67
Lya QSO	2.33	39.71 ± 0.94	8.52 ± 0.17	-0.477

accuracy is good enough, empirically. Indeed, the PAge model has been applied to many currently available data sets and yielded fruitful results (Huang 2020; Cai et al. 2022). On this basis, (Huang et al. 2021b) put forward a new model called MAPAge which provides higher measurement accuracy (Huang et al. 2021b) than the PAge model by adding a new parameter η_2 ($-1 < \eta_2 < 1$), which can be regarded as a cubic-order correction to the PAge model. In the MAPAge model, the expansion rate of the Universe is expressed as:

$$\frac{H}{H_0} = 1 + \frac{2}{3}\left(1 - (\eta + \eta_2)\frac{H_0 t}{p_{\rm age}} + \eta_2\left(\frac{H_0 t}{p_{\rm age}}\right)^2\right) \times \left(\frac{1}{H_0 t} - \frac{1}{p_{\rm age}}\right), \quad (2)$$

and Equation (2) degrades to Equation (1) when $\eta_2 = 0$.

A fitting of the Hubble parameter $H(z)$ under the redshift ($z < 10$) is applied to illustrate the advantages of MAPAge model over PAge model in model fitting, Table 1 shows the fitting accuracy of $H(z)$ among three models, it shows that the precision of MAPAge approximation is typically an order of magnitude better than PAge which is consistent with Huang et al. (2021b). The DA fitting errors of PAge and MAPAge for a few models are shown in Figure 1. The result again confirms MAPAges superiority in fitting accuracy. This is the motivation for us to choose the MAPAge model to fit current high-precision DESI data.

With the definition $H = \frac{\dot{a}}{a}$, we can express the $a(t)$ in the MAPAge model as:

$$a(t) = \left(\frac{H_0 t}{p_{\rm age}}\right)^{2/3} \exp\left(H_0 t - p_{\rm age} - \frac{2}{3}(1 + \eta + \eta_2)\left(\frac{H_0 t}{p_{\rm age}} - 1\right) + \frac{1}{3}(\eta + \eta_2)\left(\left(\frac{H_0 t}{p_{\rm age}}\right)^2 - 1\right) + \frac{\eta_2}{3}\left(\left(\frac{H_0 t}{p_{\rm age}}\right)^2 - 1\right) - \frac{2}{9}\eta_2\left(\left(\frac{H_0 t}{p_{\rm age}}\right)^3 - 1\right)\right) \quad (3)$$

The deceleration and the jerk coefficients, denoted as $q(t)$ and $j(t)$, respectively, can be obtained from the Taylor expansion of $a(t)$ at $t = t_0$:

$$a(t) = 1 + H_0(t - t_0) - \frac{1}{2}q_0 H_0^2 (t - t_0)^2 + \frac{1}{3!} j_0 H_0^3 (t - t_0)^3 + \cdots, \quad (4)$$

where we truncated the series up to a given order and used the conventional definition of the decelerating coefficient:

$$q(t) \equiv -\frac{\ddot{a}}{aH^2}, \quad q_0 \equiv q(t_0), \quad (5)$$

and the jerk coefficient:

$$j(t) \equiv \frac{\dddot{a}}{aH^3}, \quad j_0 \equiv j(t_0). \quad (6)$$

Therefore q_0 and j_0 can be expressed as functions of MAPAge parameters η, $p_{\rm age}$ and η_2 using Equations (2), (3), (5) and (6). From the MCMC fitting of the MAPAge model, we can obtain the distribution of the parameters q_0 and j_0, hence acquire the preference of the observed results for the specific model, by comparing the values of q_0 and j_0 parameters between the MAPAge model and other different models.

Table 4
The Best-fitting Values of the MAPAge Model Parameters and Its 1-σ Error Bar Obtained by MCMC Analyses

DATESET	r_d (Mpc)	$100h$ (km s^{-1} Mpc^{-1})	η	$p_{\rm age}$	η_2	q_0	j_0	$\ln L$
BAO+OHD	144	70.3 ± 2.64	0.269 ± 0.323	0.960 ± 0.0369	0.287 ± 0.487	$-0.442^{+0.272}_{-0.319}$	$0.284^{+1.672}_{-1.423}$	-12.66
	146	69.5 ± 2.57	0.279 ± 0.321	0.962 ± 0.0367	0.284 ± 0.485	$-0.454^{+0.276}_{-0.309}$	$0.329^{+1.643}_{-1.435}$	-12.08
	148	68.3 ± 2.53	0.246 ± 0.318	0.959 ± 0.036	0.329 ± 0.479	$-0.422^{+0.267}_{-0.314}$	$0.129^{+1.708}_{-1.325}$	-11.85
	150	67.5 ± 2.50	0.250 ± 0.319	0.960 ± 0.0365	0.327 ± 0.475	$-0.429^{+0.272}_{-0.309}$	$0.184^{+1.648}_{-1.379}$	-12.02
	152	66.6 ± 2.48	0.244 ± 0.317	0.960 ± 0.0364	0.337 ± 0.474	$-0.419^{+0.262}_{-0.313}$	$0.119^{+1.676}_{-1.323}$	-12.31
BAO+SNe	144	69.3 ± 0.753	0.0788 ± 0.0924	0.943 ± 0.0110	0.606 ± 0.244	$-0.305^{+0.075}_{-0.083}$	$-0.503^{+0.647}_{-0.555}$	-721.46
	146	68.3 ± 0.743	0.0804 ± 0.0929	0.943 ± 0.0110	0.604 ± 0.245	$-0.305^{+0.074}_{-0.085}$	$-0.503^{+0.666}_{-0.557}$	-721.47
	148	67.4 ± 0.728	0.0745 ± 0.0899	0.943 ± 0.0108	0.618 ± 0.238	$-0.302^{+0.072}_{-0.081}$	$-0.536^{+0.644}_{-0.536}$	-721.42
	150	66.5 ± 0.725	0.0793 ± 0.0912	0.943 ± 0.0110	0.601 ± 0.247	$-0.305^{+0.073}_{-0.082}$	$-0.501^{+0.656}_{-0.546}$	-721.43
	152	65.6 ± 0.711	0.0816 ± 0.0900	0.944 ± 0.0109	0.594 ± 0.247	$-0.309^{+0.073}_{-0.078}$	$-0.471^{+0.642}_{-0.563}$	-721.44
BAO+OHD	144	69.1 ± 0.727	0.0958 ± 0.0946	0.943 ± 0.0107	0.566 ± 0.249	$-0.317^{+0.077}_{-0.084}$	$-0.393^{+0.651}_{-0.583}$	-728.13
+SNe	146	68.2 ± 0.731	0.0961 ± 0.0950	0.943 ± 0.0110	0.562 ± 0.253	$-0.317^{+0.077}_{-0.086}$	$-0.394^{+0.676}_{-0.578}$	-727.60
	148	67.3 ± 0.708	0.0920 ± 0.0941	0.943 ± 0.0107	0.570 ± 0.248	$-0.315^{+0.077}_{-0.084}$	$-0.398^{+0.648}_{-0.597}$	-727.39
	150	66.5 ± 0.698	0.0888 ± 0.0941	0.943 ± 0.0107	0.574 ± 0.249	$-0.313^{+0.077}_{-0.084}$	$-0.430^{+0.667}_{-0.577}$	-727.49
	152	65.7 ± 0.702	0.0853 ± 0.0907	0.943 ± 0.0110	0.586 ± 0.247	$-0.310^{+0.074}_{-0.081}$	$-0.448^{+0.635}_{-0.565}$	-727.89

Note. The value of r_d ranges from 144 to 152 with a step of 2.

For subsequent purposes, it is now convenient to compute the cosmographic series for a given dark energy model. Specifically, we focus on the following models: (1) the ΛCDM model, (2) the wCDM model, and (3) the CPL model. The q_0 and j_0 expressions of these models are as follows (Luongo & Muccino 2024) (the symbols have their conventional meaning):

$$\Lambda\text{CDM:}\quad q_0 = \frac{3}{2}\,\Omega_m - 1, \quad j_0 = 1\ . \tag{7}$$

$$\begin{aligned}\text{wCDM:}\quad q_0 &= \frac{1}{2}(1 - 3\omega(\Omega_m - 1)),\\ j_0 &= \frac{1}{2}(2 - 9\omega(\Omega_m - 1)(1 + \omega)).\end{aligned} \tag{8}$$

$$\begin{aligned}\text{CPL:}\quad q_0 &= \frac{1}{2}(1 - 3\omega_0(\Omega_m - 1)),\\ j_0 &= \frac{1}{2}(2 - 9\omega_0(\Omega_m - 1)(1 + \omega_0) + 3\omega_a - 3\Omega_m\omega_a).\end{aligned} \tag{9}$$

For simplicity, these expressions did not consider energy components other than matter (Luongo & Muccino 2024). In Table 2, we exhibit q_0 and j_0 from the Planck and DESI data set calculated by Orlando Luongo and Marco Muccino as a contrast.

3. Data Analysis

The general best-fit parameters are determined directly by maximizing the total log-likelihood function:

$$\ln L = \ln L_B + \ln L_S + \ln L_O, \tag{10}$$

where the definition of L_B, L_S and L_O are introduced later in this section.

And the total BAO log-likelihood is given as:

$$\ln L_B = \sum_X \ln L_X, \tag{11}$$

where $X = d_M/r_d$, d_H/r_d, d_V/r_d, and r_d is the sound horizon at the drag epoch (Adame et al. 2024). for data about d_V, the log-likelihood represented as:

$$\ln L_{d_V} = -\frac{1}{2}\sum_{i=1}^{i=N}\left(\frac{\frac{d_V(z_i)}{r_d} - \left(\frac{d_V}{r_d}\right)_i}{(\sigma_{d_V})_i}\right)^2, \tag{12}$$

for data related to d_M and d_H, the corresponding log-likelihood can be expressed as:

$$\ln L_{d_M,d_H} = -\frac{1}{2}\sum_{i=1}^{i=N}\left(x_i^2\frac{\Delta_i}{\sigma_{d_M}^2} + y_i^2\frac{\Delta_i}{\sigma_{d_H}^2} - 2x_iy_i\frac{\Delta_i r_i}{\sigma_{d_M}\sigma_{d_H}}\right), \tag{13}$$

the parameters x, y and Δ are defined as follows:

$$\Delta_i = \frac{1}{1 - r_i^2}, \tag{14}$$

$$x_i = \frac{d_M(z_i)}{r_d} - \left(\frac{d_M}{r_d}\right)_i, \tag{15}$$

$$y_i = \frac{d_H(z_i)}{r_d} - \left(\frac{d_H}{r_d}\right)_i. \tag{16}$$

The DESI-BAO data set we used is illustrated in Table 3. Notice that the BGS and QSO tracers only provided d_V/r_d due

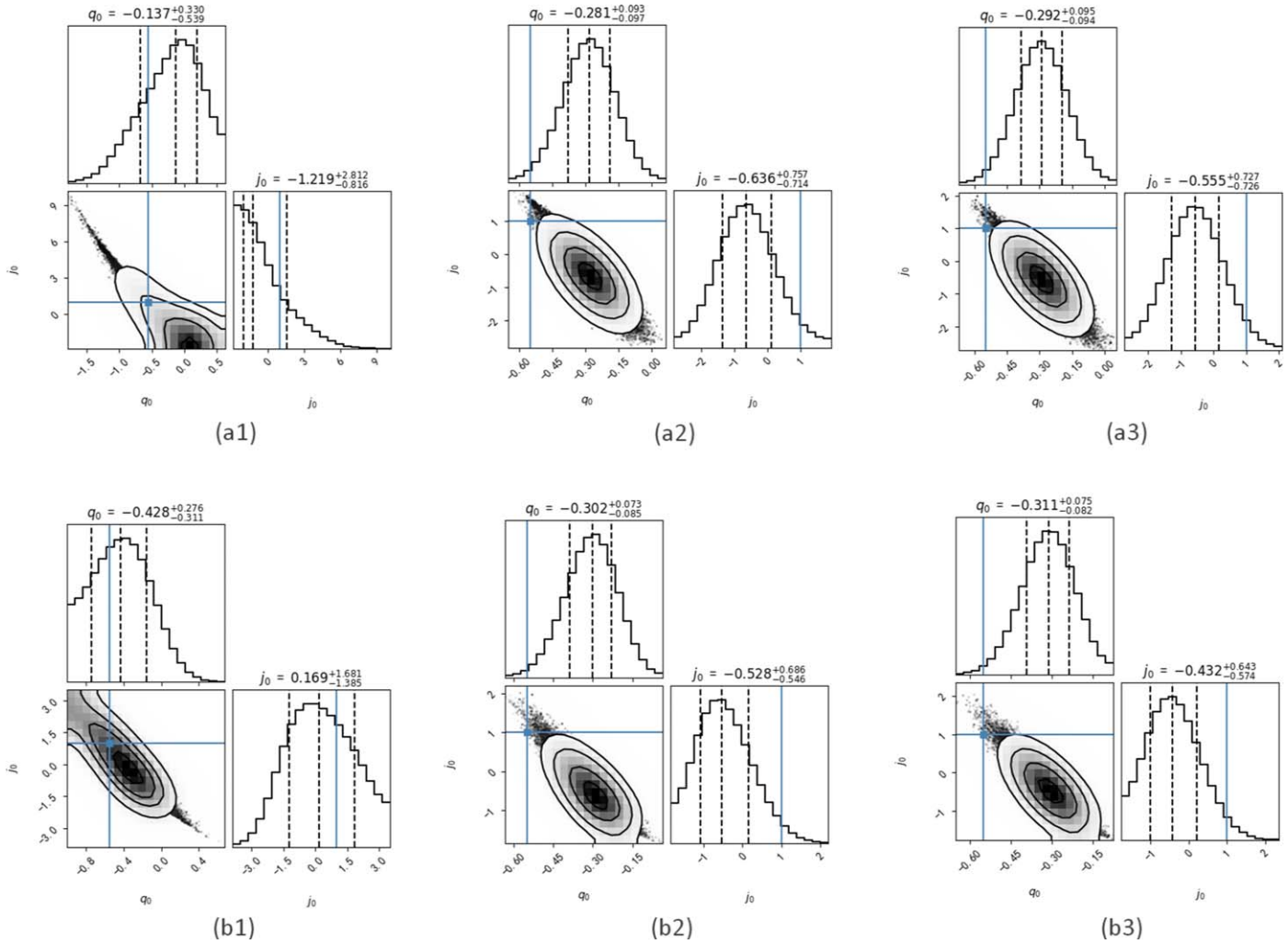

Figure 2. The total results after the MCMC analyses. The first line shows the fitting results of the CPL model, while the second line shows the results of the MAPAge model. The fitting data set used are: The first column—BAO+OHD; The second column—BAO+SNe; The third column—BAO+OHD+SNe. For each figure, $r_d = 150$. The blue point falls on $(-0.55, 1.00)$ is the theoretical calculation value of the ΛCDM model.

to the lower signal-to-noise achieved while other tracers have d_M/r_d and d_H/r_d, and provide the value of the correlation r between them but no d_V/r_d data is provided.

OHD systematics mostly depend on stellar population synthesis models and libraries. Even the initial mass functions, taken into account to calibrate the measures, together with the stellar metallicity of the population, may contribute further errors of (20–30)% (Moresco et al. 2022; Montiel et al. 2021; Muccino et al. 2023). Hence, the measures were not particularly accurate although their determination was fully model-independent. The best-fit parameters are found by maximizing the log-likelihood:

$$\ln L_O = -\frac{1}{2}\sum_{i=1}^{N_O}\left(\frac{H_i - H(z_i)}{\sigma_{H_i}}\right)^2, \tag{17}$$

and the data set of OHD we used is from Luongo & Muccino (2024) Table III.

For the supernova data, we chose the Pantheon data set, which comprises thousands of measures associated with SNe (Scolnic et al. 2018). The corresponding log-likelihood function is given by:

$$\ln L_S = -\frac{1}{2}\sum_{i=1}^{N_S}(\Delta\varepsilon_i^T C_S^{-1}\Delta\varepsilon_i + \ln(2\pi|C_S|)), \tag{18}$$

where we imposed $\Delta\varepsilon_i \equiv E_i^{-1} - E^{-1}(z_i)$ (E_i is the normalized Hubble rates), the covariance matrix C_S and its determinant $|C_S|$ (Riess et al. 2017).

4. Results and Discussion

To compare with the previous studies by Luongo & Muccino (2024), we set the comoving sound horizons at the drag epoch r_d as values vary between 144 and 152 with an even step $\delta r_d = 2$ Mpc. Table 4 shows the fitting parameters of the

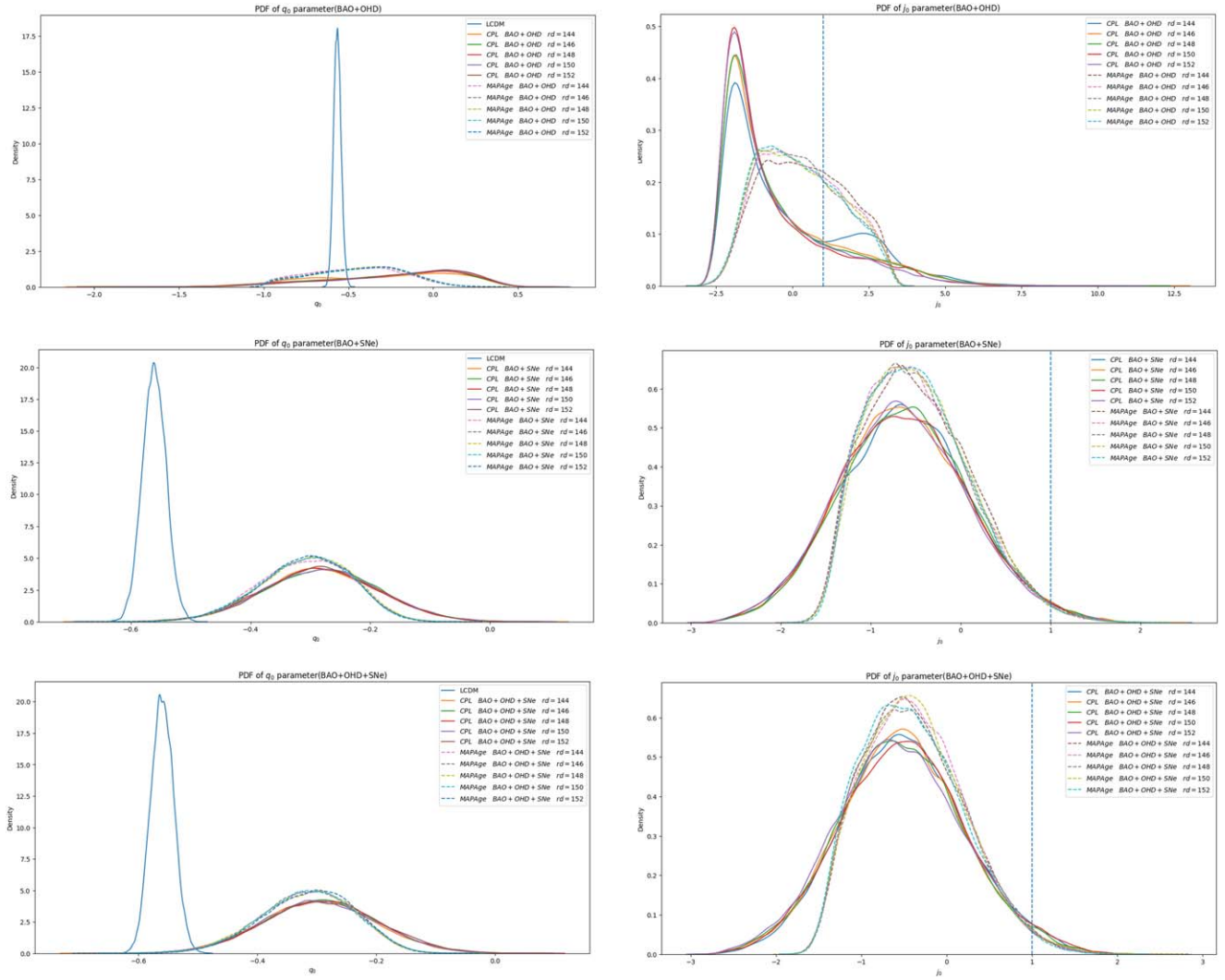

Figure 3. After adding the MCMC fitting result of LCDM, the probability density distribution is listed as the PDF of q_0 parameter on the left and the PDF of j_0 parameter on the right. According to Equation (7), j_0 of ΛCDM strictly equal to 1, it is represented by a blue vertical line in the figures on the right.

MAPAge model and the corresponding q_0 and j_0 obtained by Equations (5) and Equations (6), respectively.

The results obtained from the BAO+OHD data set are less precise and less accurate compared to those obtained from other data sets. For results obtained from the BAO+SNe and the BAO+OHD+SNe data sets, the accuracy of q_0 of the MAPAge model was consistent with the q_0 values in TABLE IV from Luongo & Muccino (2024), whereas j_0 is consistent only when s_0 is under consideration. Also, we found that h tended to decline with r_d.

Attributed to the OHD data set put a lower limitation on the parameters compared to other data sets, there is generally a larger σ when we look at q_0 and j_0 in the BAO+OHD data set. But still, all three types of measurement show an obvious inconsistency with the ΛCDM model which is exhibited in Figure 2. In order to show the gap with the ΛCDM model more strictly, we also did the same MCMC process for different data sets with the ΛCDM model and expressed results in terms of probability density function (PDF). as exhibited in Figure 3. Since the j_0 parameter in the ΛCDM model is equal to a constant: 1, so there is only a vertical line on the figures to represent j_0. But again these results show a high disagreement between the CPL model and the ΛCDM model and a high agreement between MAPAge and CPL models which once again points out the negation of the LCDM model by DESI-BAO data.

For a more detailed comparison between CPL and MAPAge, the CPL model is used to carry out the same fitting as the one done with the MAPAge model, and the corresponding results are listed in Table 5.

Table 5
The Best-Fitting Values of the CPL Model Parameters and Its 1σ Error Bar Obtained by MCMC Analyses

DATESET	r_d (Mpc)	$100h$ (km s^{-1} Mpc^{-1})	Ω_m	ω_a	ω_0	q_0	j_0	$\ln L$
BAO+OHD	144	69.3 ± 3.70	0.312 ± 0.0550	-0.962 ± 1.37	-0.763 ± 0.354	$-0.252^{+0.389}_{-0.548}$	$-0.715^{+3.120}_{-1.253}$	−12.48
	146	67.9 ± 3.47	0.297 ± 0.0889	-1.021 ± 1.43	-0.698 ± 0.331	$-0.201^{+0.380}_{-0.533}$	$-0.982^{+3.095}_{-1.028}$	−11.86
	148	67.2 ± 3.53	0.316 ± 0.0546	-1.12 ± 1.31	-0.721 ± 0.344	$-0.194^{+0.352}_{-0.537}$	$-0.965^{+2.914}_{-1.030}$	−11.53
	150	66.2 ± 3.46	0.315 ± 0.0605	-1.13 ± 1.34	-0.703 ± 0.340	$-0.174^{+0.348}_{-0.533}$	$-1.025^{+2.970}_{-0.993}$	−11.58
	152	65.1 ± 3.31	0.318 ± 0.0599	-1.25 ± 1.30	-0.676 ± 0.332	$-0.141^{+0.331}_{-0.530}$	$-1.195^{+2.895}_{-0.840}$	−11.86
BAO+SNe	144	69.3 ± 0.752	0.319 ± 0.0175	-1.09 ± 0.602	-0.763 ± 0.0810	$-0.281^{+0.094}_{-0.092}$	$-0.646^{+0.711}_{-0.701}$	−721.60
	146	68.3 ± 0.727	0.319 ± 0.0188	-1.08 ± 0.613	-0.764 ± 0.0801	$-0.282^{+0.094}_{-0.094}$	$-0.648^{+0.735}_{-0.686}$	−721.56
	148	67.4 ± 0.726	0.318 ± 0.0182	-1.07 ± 0.613	-0.765 ± 0.0814	$-0.284^{+0.094}_{-0.094}$	$-0.626^{+0.731}_{-0.707}$	−721.56
	150	66.5 ± 0.708	0.318 ± 0.0183	-1.05 ± 0.615	-0.767 ± 0.0808	$-0.287^{+0.095}_{-0.092}$	$-0.600^{+0.728}_{-0.717}$	−721.55
	152	65.6 ± 0.700	0.318 ± 0.0181	-1.08 ± 0.617	-0.764 ± 0.0825	$-0.282^{+0.095}_{-0.096}$	$-0.644^{+0.742}_{-0.707}$	−721.59
BAO+OHD	144	69.1 ± 0.726	0.318 ± 0.0218	-0.976 ± 0.624	-0.781 ± 0.0800	$-0.300^{+0.095}_{-0.094}$	$-0.504^{+0.746}_{-0.705}$	−728.25
+SNe	146	68.2 ± 0.723	0.319 ± 0.0192	-0.991 ± 0.611	-0.778 ± 0.0787	$-0.295^{+0.092}_{-0.093}$	$-0.513^{+0.723}_{-0.716}$	−727.67
	148	67.4 ± 0.704	0.319 ± 0.0196	-0.991 ± 0.614	-0.780 ± 0.0801	$-0.299^{+0.096}_{-0.091}$	$-0.510^{+0.715}_{-0.718}$	−727.47
	150	66.5 ± 0.700	0.319 ± 0.0181	-1.02 ± 0.601	-0.774 ± 0.0802	$-0.293^{+0.095}_{-0.090}$	$-0.551^{+0.708}_{-0.705}$	−727.57
	152	65.7 ± 0.690	0.319 ± 0.0187	-1.01 ± 0.611	-0.775 ± 0.0806	$-0.293^{+0.094}_{-0.094}$	$-0.552^{+0.735}_{-0.703}$	−727.94

Note. The value of r_d ranges from 144 to 152 with a step of 2.

In general, compared to $p_{\rm age}$ and η_2, the accuracy of η shows higher sensitivity to the choice of data set and j_0 shows the same case when compared with q_0. the fitting values q_0 and j_0 obtained by the two models agree with each other if including the error bars. These consistencies from the results could be supporting evidence that the MAPAge model satisfies the fundamental physical condition simply as the CPL model. However, those results that use the BAO+OHD data set show some inconsistency due to the poor quality of the BAO+OHD data set compared to other data sets. Besides, we notice that the error bars of q_0 and j_0 of the MAPAge model for specific r_d values are smaller than that of the CPL model, and the reduced Hubble parameter h obtained by the two models at specific r_d values agree with each other precisely.

In addition, there are some small but obvious differences in our results: q_0 of the MAPAge model is slightly smaller than q_0 in the CPL model. In contrast, j_0 in the CPL model is slightly smaller than j_0 in the MAPAge model. These differences could be attributed to the fact that simplified formulas were used in our calculations of q_0 and j_0.

5. Conclusion

In this work, we reconstruct the jerk parameters with DESI 2024 data, using the MAPAge model and the CPL model for fitting the data sets. The fitting results for both models are as follows: For the MAPAge model, the best-fitting results of (q_0, j_0) are approximately equal to (-0.31, -0.45). For the CPL model, the best-fitting results of (q_0, j_0) is approximately equal to (-0.30, -0.51), and the corresponding (ω_0, ω_a) is approximately equal to (-0.75, -1.00).

In comparison with the work done by Orlando Luongo and Marco Muccino, our approach ensures a set of physical conditions are fulfilled, and the parameters in the MAPAge model show a higher accuracy level than the CPL model. Our results are consistent with the CPL model but show deviation from the standard ΛCDM model, which once again proves the inconsistency of the new DESI data with the standard model.

Acknowledgments

This work is supported by the National SKA Program of China No. 2020SKA0110402, the National Natural Science Foundation of China (NSFC) general program (grant No. 12073088), and the National Key R&D Program of China (grant No. 2020YFC2201600), and Guangdong Basic and Applied Basic Research Foundation (grant No. 2024A1515012573).

ORCID iDs

Kun-Yuan Hong https://orcid.org/0009-0003-8256-5178

References

Adame, A., Aguilar, J., Ahlen, S., et al. 2024, arXiv:2404.03002
Aghanim, N., Akrami, Y., Ashdown, M., et al. 2020, A&A, 641, A6
Bamba, K., Capozziello, S., Nojiri, S., & Odintsov, S. D. 2012, Ap&SS, 342, 155
Baumann, D. 2009, arXiv:0907.5424
Brieden, S., Gil-Marín, H., & Verde, L. 2023, JCAP, 2023, 023
Cai, R.-G., Guo, Z.-K., Wang, S.-J., Yu, W.-W., & Zhou, Y. 2022, PhRvD, 106, 063519
Calderon, R., Lodha, K., Shafieloo, A., et al. 2024, JCAP, 2024, 048
Carloni, Y., Luongo, O., & Muccino, M. 2024, arXiv:2404.12068
Colgáin, E. Ó, Dainotti, M. G., Capozziello, S., et al. 2024, arXiv:2404.08633
Di Valentino, E., Mena, O., Pan, S., et al. 2021, CQGra, 38, 153001

Eisenstein, D. J., & Hu, W. 1998, ApJ, 496, 605
Hu, J.-P., & Wang, F.-Y. 2023, Univ, 9, 94
Huang, L., Huang, Z., Luo, X., He, X., & Fang, Y. 2021a, PhRvD, 103, 123521
Huang, L., Huang, Z.-Q., Li, Z.-Y., & Zhou, H. 2021b, RAA, 21, 277
Huang, Z. 2020, ApJL, 892, L28
Huang, Z., Liu, J., Mo, J., et al. 2024, arXiv:2405.03983
Luo, X., Huang, Z., Qian, Q., & Huang, L. 2020, ApJ, 905, 53
Luongo, O., & Muccino, M. 2024, arXiv:2404.07070
Marina, C., Liddle, A. R., et al. 2024, arXiv:2404.08056
Montiel, A., Cabrera, J., & Hidalgo, J. C. 2021, MNRAS, 501, 3515
Moresco, M., Amati, L., Amendola, L., et al. 2022, LRR, 25, 6
Muccino, M., Luongo, O., & Jain, D. 2023, MNRAS, 523, 4938
Perivolaropoulos, L., & Skara, F. 2022, NewAR, 95, 101659
Riess, A. G., Rodney, S. A., Scolnic, D. M., et al. 2017, ApJ, 853, 126
Riess, A. G., Yuan, W., Macri, L. M., et al. 2022, ApJL, 934, L7
Scolnic, D. M., Jones, D., Rest, A., et al. 2018, ApJ, 859, 101
Visser, M. 2004, CQGra, 21, 2603
Yang, Y., Ren, X., Wang, Q., et al. 2024, SciBu, 69, 2698